Effect of Substituents on the GPx-like Activity of Ebselen: Steric versus Electronic

Jason K. Pearson and Russell J. Boyd*

Department of Chemistry, Dalhousie University, Halifax, Nova Scotia, Canada B3H 4J3

Received: August 9, 2007; In Final Form: November 14, 2007

The direct oxidation of ebselen and several derivatives by hydrogen peroxide is investigated using the B3LYP/6-31G(d,p) method to elucidate the effects of substituents on GPx-like activity. While previous studies have attributed the differences in GPx activity of substituted ebselen compounds to the electronic nature of the substituents, the influence of functional groups is poorly understood. The effects of various solvents are incorporated by employing the CPCM method. It is shown that a substituent in the ortho position to the selenium atom sterically hinders attack of a nucleophile at selenium and thus increases the barrier to reaction. The observed increase in GPx-like activity of an ebselen derivative with an ortho substituent is explained by the fact that the steric hindrance prevents thiol exchange reactions.

Introduction

Oxidative stress caused by peroxides and other reactive oxygen species has been implicated in a wide variety of degenerative human conditions including various disease states and even the process of aging.[1,2] This provides strong motivation to develop novel and effective antioxidants to combat such species. Ebselen (**1**) (2-phenyl-1,2-benzisoselenazol-3(2*H*)-one) is an antioxidant and glutathione peroxidase (GPx) mimic[3−8] that has attracted much interest because of its anti-inflammatory, antiatherosclerotic, and cytoprotective properties in both in vitro and in vivo models.[9−14]

The active form of ebselen is the selenol (**3**),[15−19] which is produced via reaction with 2 equiv of thiol: the first cleaving the selenamide bond (i.e., **1** → **2**) and the second cleaving the resultant selenosulfide bond (i.e., **2** → **3**).The GPx-like mechanism of ebselen is therefore given by the route **3** → **4** → **2**. This process is complicated by the fact that for the selenosulfide (**2**), an incoming thiol prefers to attack the more electrophilic selenium atom as shown by Mugesh,[20] resulting in a thiol exchange reaction and no net catalytic activity. Interestingly, the addition of a nitro group ortho to selenium yields more than a 9-fold increase in GPx activity.[21] This marked increase has been attributed to electronic effects;[22] however, the influence of the functional group is poorly understood. The attribution of the differences in observed GPx activities to electronic or other effects is not trivial. The current work demonstrates that the incorporation of a substituent ortho to selenium induces a steric effect that inhibits the approach of nucleophiles at selenium for the direct oxidation reaction (**1** → **6**). It is postulated that this steric effect must also be present for the reaction of the selenosulfide intermediate with a thiol (**2** → **3**) and therefore helps to overcome thiol exchange. It is proposed that this is the basis for the increased activity of the ortho-substituted ebselen compound.

Computational Methods

All geometry optimizations and single-point energy calculations were carried out with the Gaussian 03[23] software package.

* Corresponding author. E-mail: russell.boyd@dal.ca.

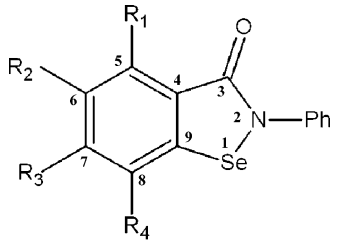

(a) R_1, R_2, R_3, R_4 = H
(b) R_1 = H, R_2 = NO_2, R_3, R_4 = H
(c) R_1, R_2, R_3 = F, R_4 = H
(d) R_1, R_2, R_3 = H, R_4 = NO_2
(e) R_1, R_2, R_3 = H, R_4 = HCO
(f) R_1, R_2, R_3 = H, R_4 = *t*-but
(g) R_1, R_2, R_3 = H, R_4 = OCH_3

Figure 1. Series of structures studied in this paper.

Optimizations were performed with Becke's three-parameter exchange functional[24] (B3) in combination with the correlation functional of Lee, Yang, and Parr[25] (LYP) in conjunction with the 6-31G(d,p) Pople basis set, which was shown to be reliable for the prediction of organoselenium geometries and energetics in a previous paper.[26] Transition states were located using Schlegel's synchronous transit-guided quasi-Newton (STQN) method[27,28] and were linked to reactant and product complex structures by the use of intrinsic reaction coordinate calculations.[29,30] Properties of each system in solution were obtained with the conductor-like polarizable continuum model (CPCM) employed with the B3LYP/6-31G(d,p) method at the gas-phase geometry. The topology of the electron density was examined with the AIM2000[31] and AIMPAC[32] software packages using the appropriate gas-phase or solution-phase wave functions.

Results and Discussion

Gas-Phase GPx-like Activity. Gas-phase transition structures for the direct oxidation of ebselen (i.e., **1** → **6**) and several analogues (Figure 1) by hydrogen peroxide were located, and the relevant computed properties are summarized in Table 1. $\Delta E_e^{\ddagger}$ refers to the difference in the gas-phase electronic energy between the transition state (TS) and reactant complex (RC) although the qualitative trend is identical if one considers the

10.1021/jp076404w CCC: $40.75
Published on Web 01/16/2008

TABLE 1: Gas-Phase Electronic Energy Barriers ($\Delta E_e^{\ddagger}$), Electronic Charges on Selenium (q_{Se}), and Changes in Electronic Charge on Selenium and Each Peroxide Oxygen Atom ($\Delta q_{Se}^{(TS-RC)}$, $\Delta q_{O1}^{(TS-RC)}$, and $\Delta q_{O2}^{(TS-RC)}$) for the Direct Oxidation of Ebselen and Several Derivatives by Hydrogen Peroxide[a]

structure	$\Delta E_e^{\ddagger}$ (kcal/mol)	q_{Se} (e)	$\Delta q_{Se}^{(TS-RC)}$ (e)	$\Delta q_{O1}^{(TS-RC)}$ (e)	$\Delta q_{O2}^{(TS-RC)}$ (e)	∠OOSeC (deg)	∠CCSeO (deg)
a	25.7	0.57	0.36	−0.25	−0.25	−93.3	35.5
b	27.8	0.61	0.33	−0.25	−0.25	−93.3	35.1
c	26.6	0.60	0.34	−0.25	−0.26	−90.6	34.8
d	34.0	0.74	0.37	−0.23	−0.25	−128.2	81.1
e	33.1	0.71	0.37	−0.23	−0.26	−130.9	80.6
f	30.9	0.55	0.38	−0.23	−0.28	−122.0	68.5
g	30.9	0.57	0.37	−0.23	−0.27	−106.2	55.1

[a] O1 corresponds to the selenoxide oxygen atom, and O2 corresponds to the oxygen atom in the resultant water molecule. ∠OOSeC and ∠CCSeO are the dihedral angles in the TS of each species (in deg). OOSeC corresponds to atoms O1, O2, Se(1), and C(9), while CCSeO corresponds to atoms C(8), C(9), Se(1), and O1. The Se and C atoms are numbered according to Figure 1.

SCHEME 1

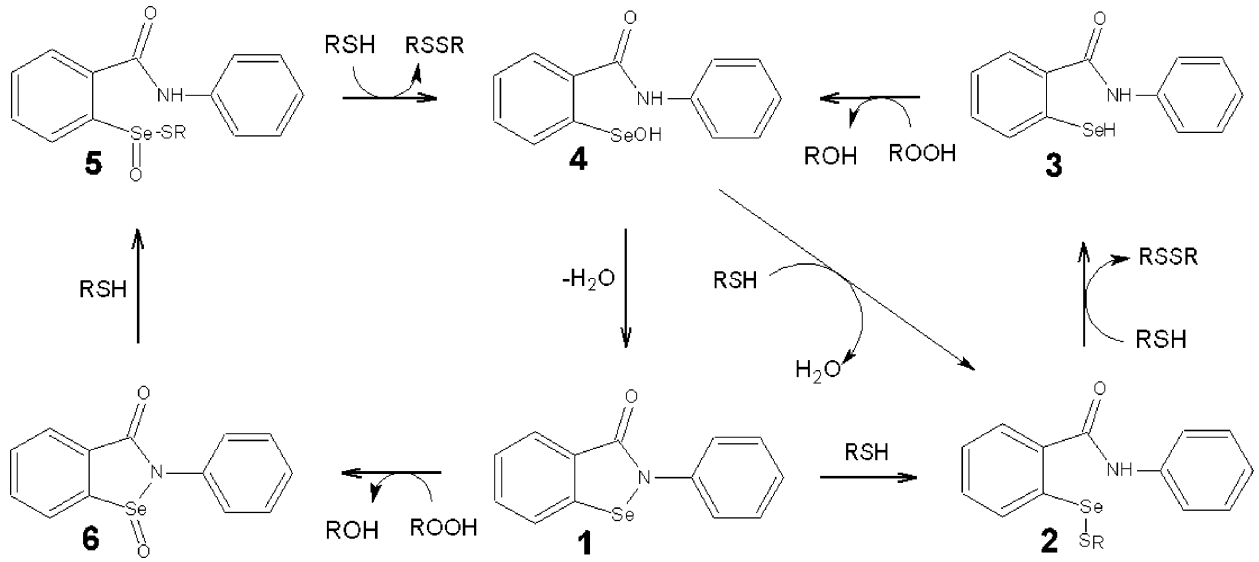

difference in energy between the TS and the infinitely separated reactants. It is shown that the barrier increases by over 30% upon the addition of a nitro substituent at the ortho position (i.e., **d**, $R_4 = NO_2$); however, when the same substituent is in the para position (i.e., **b**, $R_2 = NO_2$), the barrier is only slightly greater than that of the unsubstituted case. If one calculates the barrier for a system with different electronic properties but essentially identical sterics (**e**), it is again found that the barrier is elevated by ∼30%. The search for the TS with compound **e** was restricted in the sense that the O atom of the HCO group was oriented toward the peroxide molecule as a starting point instead of the H atom to maintain the steric environment about the Se atom of compound **d**. The TS optimization however was not restricted, and the TS obtained is a true transition state of the system. A similar barrier elevation is observed for systems to which electron-donating substituents are incorporated, such as a bulky *tert*-butyl group (**f**) or a methoxy group (**g**). Compound **g**, like compound **e,** was also oriented so as to create a more sterically hindered environment as a starting point for the optimization. Incorporating electronegative fluorine atoms (**c**) is another modification to the electronic nature of the selenium heterocycle that maintains the steric environment of the original ebselen molecule yet this system shows a barrier that is the same as that of ebselen. These data demonstrate that a substituent in the ortho position to selenium causes an increase in the barrier to oxidation by hydrogen peroxide, yet various modifications to the electronic nature of the selenium heterocycle have little or no effect.

The charge on the selenium atom in the isolated molecules, q_{Se}, is also presented in Table 1 along with the change in electronic charge on the selenium atom and each peroxide oxygen atom as the species go from the RC to the TS ($\Delta q_{Se}^{(TS-RC)}$, $\Delta q_{O1}^{(TS-RC)}$, and $\Delta q_{O2}^{(TS-RC)}$). It has been shown in a previous paper that these three atoms dominate the charge transfer and energy profiles of such reactions.[19] These data show that although the substituents do affect the electron density of selenium (as seen by the differences in q_{Se}), they have virtually no effect on electronic transfer during the course of the reaction, and therefore the difference in reactivity cannot be ascribed to electronic effects. The result is, then, a steric effect, which leads to a less-than-optimal alignment between the peroxide nucleophile and the substrate selenium atom in the TS. This is shown graphically in Figure 2.

The dihedral angles presented in Table 1 in conjunction with Figure 2 illustrate the change in the position of the hydrogen peroxide molecule in the TS upon incorporating a substituent in the ortho position (R_4 = HCO shown). The peroxide orientation is significantly altered, and this is reflected in the barrier to reaction.

At this point it is prudent to consider the possibility of the influence of the potential hydrogen bond acceptors within the R_4 substituents to the results in Table 1 (i.e., reaction barriers, etc.). While structures **d**, **e**, and **g** all contain potential hydrogen bond acceptors, the molecular graphs obtained using Bader's QTAIM technique show no bond paths between the peroxide

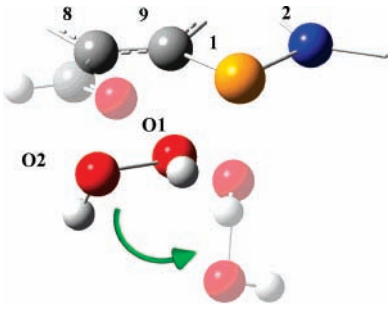

Figure 2. Partial transition state structures of the direct reduction of hydrogen peroxide by molecules **a** and **e**, illustrating the steric effect induced by an ortho substituent to the selenium atom. The faded peroxide molecule corresponds to the orientation when there is a substituent in the R_4 position.

hydrogen atoms and the R_4 substituent, ruling out any possible H-bond formation (Figure 3). The RC structures of both **d** and **e** do show a bond path between a peroxide oxygen and an oxygen of the ortho substituent (only that of **d** is shown); however, the electron density at the bond critical point (ρ_{BCP}) of these bonds (0.005 au) is roughly 2 orders of magnitude lower than that of the peroxide O−O bond (0.277 au), indicating a negligible interaction. Although one may expect a rotation of the HCO substituent in **e** to orient the H toward the peroxide instead of the O, this case has not been investigated because it does not mimic the steric environment of the ortho NO_2 case (**d**) and thus will not aid in deducing the electronic or steric reason for its increased reactivity with respect to the unsubstituted case. It is postulated that the basis for the experimentally observed increase in GPx-like activity of **d** is due to sterics, and thus it is convenient to compare results with a structure that can provide almost exactly the same steric environment but with different electronic properties. The HCO substituent fills this criterion but only in the particular conformation that orients the O atom toward the incoming peroxide molecule.

Similarly, the RC of **g** shows a bond path between the methoxy H and the nearest peroxide O. This is also a weak interaction with a ρ_{BCP} of ~0.006 au. The TS of **g** also exhibits bond paths between the R_4 substituent and the peroxide oxygen atoms having electron densities of ~0.015 au at each bond critical point. While these bond critical points have a higher electron density than the case for the RC, it is still significantly smaller than a typical O−H bond critical point density of 0.3 au; thus, it can also be considered a negligible interaction, and thus hydrogen bonding does not influence the behavior of the reactions studied here.

Solvent Effects on GPx-like Activity. When investigating the properties of molecules in a biological context, it becomes imperative to incorporate the effect of an aqueous environment into the calculation. Initially this was completed by performing single-point energy calculations on the gas-phase optimized geometries of each species using the CPCM method with a water solvent. The solution-phase wave functions were then used to calculate atomic properties of each species in solution. The qualitative trends in the resultant solution-phase barriers, however, did not agree with those of the gas phase. That is, there was no clear relationship between the position of the substituent relative to the selenium atom and the electronic barrier to reaction. To probe the effect of solvent further, the calculations were repeated with a series of solvents having a wide range of dielectric constants, which would allow for a "tuning" of the solvent effect. This would afford the opportunity to observe precisely how the solvent changes the behavior of these systems.

Figure 4 illustrates the barriers to reaction (in kcal/mol) for each molecular species in a series of seven environments including the gas phase. The data at the far right indicate the aqueous results ($\epsilon = 78.39$), while the data at the far left indicate that of the gas phase ($\epsilon = 1$) from Table 1. The series are color coded according to whether or not the system has a substituent in the ortho position to the selenium atom (i.e., a substituent in the R_4 position) to illustrate the stark contrast in the trend of gas-phase barriers vs those in an aqueous environment. In general, as the dielectric constant is increased, the barriers of **a**, **b**, and **c** also increase, but the barriers of **d**, **e**, **f**, and **g** decrease. This results in a "mixing" of barriers where in gas phase there were two distinct groups.

In addition to the gas-phase data, there are clearly two distinct groups in the context of the entire data set. The ortho-substituted derivatives respond similarly to a change in external dielectric but distinctly from the other species and vice versa. Compounds **a**, **b**, and **c** are more sensitive to a change in external dielectric as shown by a steeper profile in Figure 4. The interaction of the CPCM solvent with the system is via many point charges distributed over the surface of a molecular cavity. The interaction energy between the static charge distribution of the system and some external charge is quantified by the electrostatic potential of the system, which is a real physical property defined by[33]

$$V^{ES}(\mathbf{r}) = \sum_A \frac{Z_A}{|\mathbf{R}_A - \mathbf{r}|} - \int \frac{\rho(\mathbf{r}')\, d\mathbf{r}'}{|\mathbf{r}' - \mathbf{r}|} \qquad (1)$$

In (1) Z_A is the charge on nucleus A, located at $\mathbf{R}_A$, and $\rho(\mathbf{r}')$ is the electron density at $\mathbf{r}'$.

The electrostatic potential then is a tool capable of assessing the basis for a difference in behavior as a result of an external dielectric from the CPCM solvent model. Figure 5 illustrates three-dimensional isosurfaces of the electrostatic potential for the transition states of **a** and **d**. (These two systems are representative of the two types of species studied, one with and one without a substituent ortho to the selenium atom.) It is clear that the major difference between the two lies in the negative potential surrounding the reacting peroxide molecule. This is also precisely the region that dominates the energy profile of the reaction, and thus the barrier is sensitive to an external dielectric. Because the systems **a** through **g** essentially exhibit only two distinct electrostatic potentials (those with a substituent ortho to the selenium atom and those without), their sensitivities to the CPCM solvent model are correspondingly similar, and therefore there are two distinct groups in Figure 4.

The negative electrostatic potential generated from a fictitious system in which the peroxide orientation of **d** is imposed upon the substrate structure of **a** is identical to that of **d**. Therefore, the nature of the negative electrostatic potential is not directly due to the substituent but rather the orientation of the peroxide molecule, although this orientation *is* due to the substituent.

These data show that there is indeed a steric effect at play in the direct oxidation of molecules **a** through **g** by hydrogen peroxide which is complicated by an influence from the solvent. A substituent ortho to the selenium atom in these systems changes the approach angle of the peroxide nucleophile, which has a direct effect on the barrier to reaction as well as the change in barrier due to varying the solvent medium.

Recently, it has been suggested that a solvent-assisted proton exchange (SAPE) mechanism is required to accurately predict

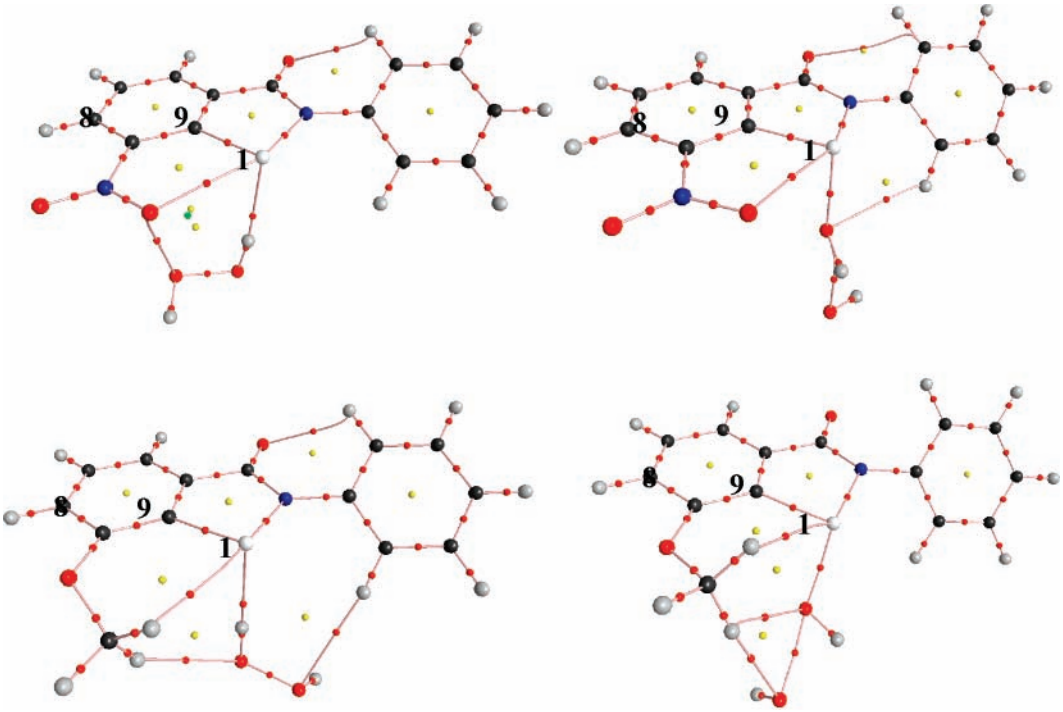

Figure 3. QTAIM molecular graphs of the RC (left) and TS (right) of **d** (top) and **g** (bottom).

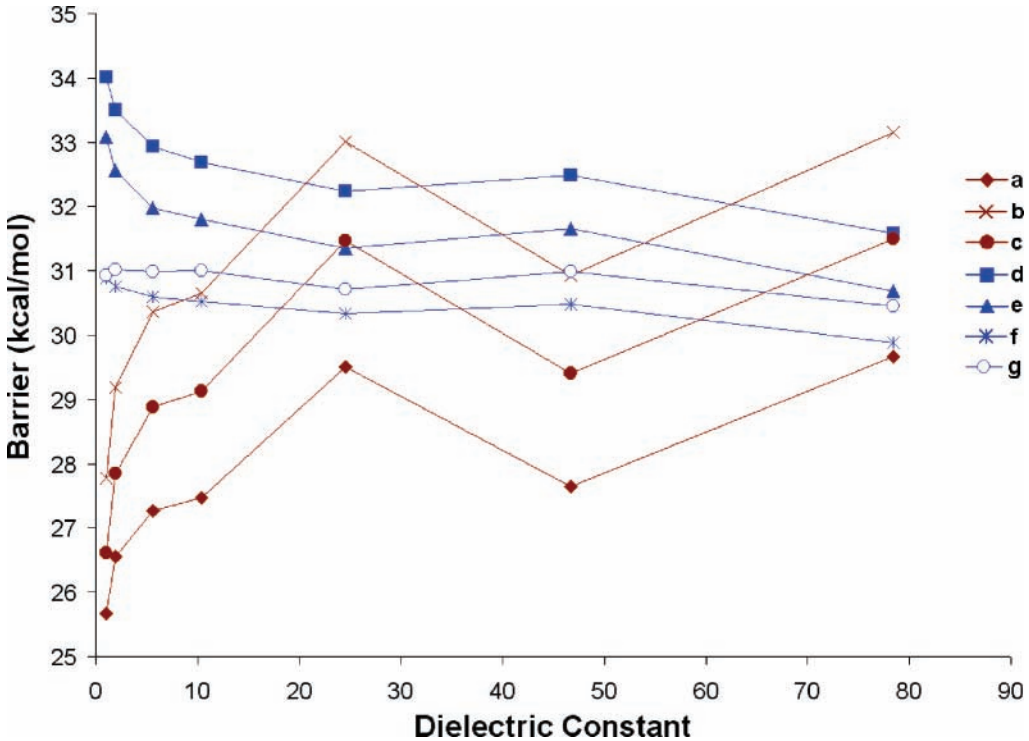

Figure 4. Electronic energy barriers for the direct oxidation of **a**−**g** with respect to the dielectric constant of the CPCM solvent. The solvents employed are heptane ($\epsilon = 1.92$), chlorobenzene ($\epsilon = 5.62$), dichloroethane ($\epsilon = 10.36$), ethanol ($\epsilon = 24.55$), DMSO ($\epsilon = 46.7$), and water ($\epsilon = 78.39$). The gas-phase results are also included. The blue series indicate molecules that have a substituent ortho to the selenium atom. All data calculated at the B3LYP/6-31G(d,p) level.

reasonable barriers for such processes.[34] Such an approach involves explicitly solvating the reactant species to provide a lower energy pathway by allowing a concerted series of proton exchanges via the solvent, and thus a 1,2 proton shift on the peroxide is not necessary. This has been shown to reduce the theoretically predicted barriers. While it is possible to employ SAPE in the current work to reduce the theoretically predicted barriers, it is not likely that this effect would alter the reported trends, and thus no new conclusions would be drawn as to the nature of the GPx-like activity of these compounds. In fact, one could imagine that the SAPE network of solvent molecules would also be sterically inhibited by substituents in the R_4 position, and thus the steric effect reported herein would be amplified.

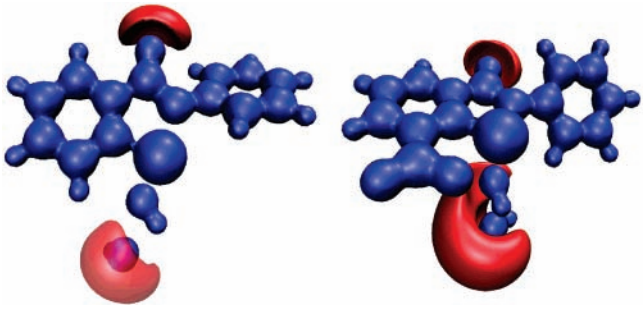

Figure 5. Electrostatic potential diagrams for the transition state structures of ebselen (a) on the left and the ortho-nitro-substituted ebselen (d) on the right. The blue isosurface corresponds to an electrostatic potential of 0.6 au while the red isosurface corresponds to an electrostatic potential of −0.06 au. Some of the negative isosurface of **a** has been faded to show the underlying positive potential.

Conclusions

Experimentally, a nitro group in the ortho position to the selenium atom in ebselen produces more than a 9-fold increase in its GPx-like activity. Although Table 1 shows a higher barrier for this case, the experimentally suggested route is via the selenosulfide intermediate (i.e., **1** → **2** → **3** → **4**) and not via direct oxidation. The conversion of this intermediate to the selenol (**2** → **3**) is complicated, however, by a thiol exchange reaction whereby a thiol nucleophile attacks the more positive selenium center, and thus no net reaction occurs.[20] Considering thiol exchange, these results strongly suggest that the ortho substituent hinders attack of the thiol at selenium and promotes production of the selenol, the GPx-active form, and thus the GPx-like activity is greatly enhanced. On the basis of these results, one can now produce more active GPx mimics than ebselen by overcoming thiol exchange using ortho substituents. The electronic nature of these substituents is much less important than their steric bulk but clearly the solvent plays an important role. An optimal GPx mimic would employ an ortho substituent to inhibit approach of thiol at the selenium center yet still have a low barrier to facilitate the entire redox cycle. This makes compound **f** the clear choice due to its steric bulk but relatively low barrier to oxidation in an aqueous medium.

Acknowledgment. The authors thank Jean Burnell and Erin Johnson for thoughtful discussions as well as the Natural Sciences and Engineering Research Council of Canada for financial support. J.K.P. also thanks the Killam Trusts for financial support.

Supporting Information Available: Archive entries for all optimizations (Table S1). This information is available free of charge via the Internet at http://pubs.acs.org.

References and Notes

(1) *Free Radicals in Biology*; Pryor, W. A., Ed.; Academic Press: New York, 1982; Vol. 5, p 283.

(2) *Free Radicals in Molecular Biology, Aging, and Disease*; Armstrong, D., Sohal, R. S., Cutler, R. G., Slater, T. F., Eds.; Raven Press: New York, 1984; Vol. 27, p 416.

(3) Müller, A.; Cadenas, E.; Graf, P.; Sies, H. *Biochem. Pharmacol.* **1984**, *33*, 3235.

(4) Wendel, A.; Fausel, M.; Safayhi, H.; Tiegs, G.; Otter, R. *Biochem. Pharmacol.* **1984**, *33*, 3241.

(5) Parnham, M. J.; Kindt, S. *Biochem. Pharmacol.* **1984**, *33*, 3247.

(6) Müller, A.; Gabriel, H.; Sies, H. *Biochem. Pharmacol.* **1985**, *34*, 1185.

(7) Safayhi, H.; Tiegs, G.; Wendel, A. *Biochem. Pharmacol.* **1985**, *34*, 2691.

(8) Wendel, A.; Tiegs, G. *Biochem. Pharmacol.* **1986**, *35*, 2115.

(9) Fong, M. C.; Schiesser, C. H. *Tetrahedron Lett.* **1995**, *36*, 7329.

(10) Sies, H. *Free Radical Biol. Med.* **1993**, *14*, 313.

(11) Sies, H. *Methods Enzymol.* **1994**, *234*, 476.

(12) Schewe, T. *Gen. Pharmacol.* **1995**, *26*, 1153.

(13) Nakamura, Y.; Feng, Q.; Kumagai, T.; Torikai, K.; Ohigashi, H.; Osawa, T.; Noguchi, N.; Niki, E.; Uchida, K. *J. Biol. Chem.* **2002**, *277*, 2687.

(14) Zhang, M.; Nomura, A.; Uchida, Y.; Iijima, H.; Sakamoto, T.; Iishii, Y.; Morishima, Y.; Mochizuki, M.; Masuyama, K.; Hirano, K.; Sekizawa, K. *Free Radical Biol. Med.* **2002**, *32*, 454.

(15) Zhao, R.; Holmgren, A. *J. Biol. Chem.* **2002**, *277*, 39456.

(16) Maiorino, M.; Roveri, A.; Coassin, M.; Ursini, F. *Biochem. Pharmacol.* **1988**, *37*, 2267.

(17) Morgenstern, R.; Cotgreave, I. A.; Engman, L. *Chem.-Biol. Interact.* **1992**, *84*, 77.

(18) Cotgreave, I. A.; Moldeus, P.; Brattsand, R.; Hallberg, A.; Andersson, C. M.; Engman, L. *Biochem. Pharmacol.* **1992**, *43*, 793.

(19) Pearson, J. K.; Boyd, R. J. *J. Phys. Chem. A* **2007**, *111*, 3152.

(20) Sarma, B. K.; Mugesh, G. *J. Am. Chem. Soc.* **2005**, *127*, 11477.

(21) Parnham, M. J.; Biedermann, J.; Bittner, C.; Dereu, N.; Leyck, S.; Wetzig, H. *Agents Actions* **1989**, *27*, 306.

(22) Mugesh, G.; du Mont, W.-W.; Sies, H. *Chem. Rev.* **2001**, *101*, 2125.

(23) Frisch, M. J.; Trucks, G. W.; Schlegel, H. B.; Scuseria, G. E.; Robb, M. A.; Cheeseman, J. R.; J. A. Montgomery, J.; Vreven, T.; Kudin, K. N.; Burant, J. C.; Millam, J. M.; Iyengar, S. S.; Tomasi, J.; Barone, V.; Mennucci, B.; Cossi, M.; Scalmani, G.; Rega, N.; Petersson, G. A.; Nakatsuji, H.; Hada, M.; Ehara, M.; Toyota, K.; Fukuda, R.; Hasegawa, J.; Ishida, M.; Nakajima, T.; Honda, Y.; Kitao, O.; Nakai, H.; Klene, M.; Li, X.; Knox, J. E.; Hratchian, H. P.; Cross, J. B.; Adamo, C.; Jaramillo, J.; Gomperts, R.; Stratmann, R. E.; Yazyev, O.; Austin, A. J.; Cammi, R.; Pomelli, C.; Ochterski, J. W.; Ayala, P. Y.; Morokuma, K.; Voth, G. A.; Salvador, P.; Dannenberg, J. J.; Zakrzewski, V. G.; Dapprich, S.; Daniels, A. D.; Strain, M. C.; Farkas, O.; Malick, D. K.; Rabuck, A. D.; Raghavachari, K.; Foresman, J. B.; Ortiz, J. V.; Cui, Q.; Baboul, A. G.; Clifford, S.; Cioslowski, J.; Stefanov, B. B.; Liu, G.; Liashenko, A.; Piskorz, P.; Komaromi, I.; Martin, R. L.; Fox, D. J.; Keith, T.; Al-Laham, M. A.; Peng, C. Y.; Nanayakkara, A.; Challacombe, M.; Gill, P. M. W.; Johnson, B.; Chen, W.; Wong, M. W.; Gonzalez, C.; Pople, J. A. *Gaussian 03, Revision B.05*; Gaussian Inc.: Pittsburgh, 2003.

(24) Becke, A. D. *J. Chem. Phys.* **1993**, *98*, 1372.

(25) Lee, C. T.; Yang, W. T.; Parr, R. G. *Phys. Rev. B* **1988**, *37*, 785.

(26) Pearson, J. K.; Ban, F.; Boyd, R. J. *J. Phys. Chem. A* **2005**, *109*, 10373.

(27) Peng, C. Y.; Schlegel, H. B. *Isr. J. Chem.* **1993**, *33*, 449.

(28) Peng, C. Y.; Ayala, P. Y.; Schlegel, H. B.; Frisch, M. J. *J. Comput. Chem.* **1996**, *17*, 49.

(29) Gonzalez, C.; Schlegel, H. B. *J. Chem. Phys.* **1989**, *90*, 2154.

(30) Gonzalez, C.; Schlegel, H. B. *J. Phys. Chem.* **1990**, *94*, 5523.

(31) Biegler-König, F.; Schönbohm, J.; Bayles, D. *J. Comput. Chem.* **2001**, *22*, 545.

(32) The AIMPAC suite of programs may be downloaded from Richard Bader's Web site: www.chemistry.mcmaster.ca/bader.

(33) *Chemical Applications of Atomic and Molecular Electrostatic Potentials*; Truhlar, D., Politzer, P., Eds.; Plenum Press: New York, 1981.

(34) Bayse, C. A. *J. Phys. Chem. A* **2007**, *111*, 9070.